Effects of Chromogranin Expression on Inositol 1,4,5-Trisphosphate-Induced Intracellular Ca^{2+} Mobilization

Yang Hoon Huh, Soung Hoo Jeon,§ Jie Ae Yoo, Seon Young Park, and Seung Hyun Yoo*

National Creative Research Initiative Center for Secretory Granule Research and Department of Biochemistry, Inha University College of Medicine, Jung Gu, Incheon 400-712, Korea

Received September 8, 2004; Revised Manuscript Received January 17, 2005

ABSTRACT: We show here that expression of chromogranins in non-neuroendocrine NIH3T3 cells significantly increased the amount of IP_3-mediated intracellular Ca^{2+} mobilization in these cells, whereas suppression of them in neuroendocrine PC12 cells decreased the amount of mobilized Ca^{2+}. We have therefore investigated the relationship between the IP_3-induced intracellular Ca^{2+} mobilization and secretory granules. The level of IP_3-mediated Ca^{2+} release in CGA-expressing NIH3T3 cells was 40% higher than in the control cells, while that of CGB-expressing cells was 134% higher, reflecting the number of secretory granules formed. Suppression of CGA and CGB expression in PC12 cells resulted in 41 and 78% reductions in the number of secretory granules, respectively, while the extents of IP_3-induced Ca^{2+} release in these cells were reduced 40 and 69%, respectively. The newly formed secretory granules of NIH3T3 cells contained all three isoforms of the IP_3Rs. Comparison of the concentrations of the IP_3R isoforms expressed in the ER and nucleus of chromogranin-expressing and nonexpressing NIH3T3 cells did not show significant differences, indicating that chromogranin expression did not affect the expression of endogenous IP_3Rs. Nonetheless, the IP_3R concentrations in secretory granules of chromogranin-expressing NIH3T3 cells were 3.5−4.7-fold higher than those of the ER, similar to the levels found in secretory granules of neuroendocrine chromaffin cells, thus suggesting that the IP_3Rs targeted to the newly formed secretory granules are newly induced by chromogranins without affecting the expression of intrinsic IP_3Rs. These results strongly suggest that the extent of IP_3-induced intracellular Ca^{2+} mobilization in secretory cells is closely related to the number of secretory granules.

Chromogranins A and B are major proteins of secretory granules of neuroendocrine cells (*1*−*4*); thus, they are called marker proteins of neuroendocrine cells (*5*). In addition to the abundance of chromogranins, secretory granules of neurons, exo/endocrine cells, and neuroendocrine cells (secretory cells) contain 40 mM Ca^{2+} (*6*, *7*) and store up to 60% of intracellular calcium (*8*). Most (>99.9%) of the intragranular Ca^{2+} stays bound to chromogranins in secretory granules (*9*), and only a very small portion (<0.1%) of the granular Ca^{2+} exists in the free state (*9*−*13*). Hence, chromogranins are also called Ca^{2+} storage proteins: chromogranin A binds 32−55 mol of Ca^{2+}/mol with a dissociation constant (K_d) of 2.7−4 mM (*14*), while chromogranin B binds ∼90 mol of Ca^{2+}/mol with a K_d of 1.5 mM (*15*).

Chromogranins A and B interact with the IP_3R at the intragranular pH of 5.5 and activate the inositol 1,4,5-trisphosphate receptor/Ca^{2+} channel (*16*), drastically increasing the open probability and the mean open time of the channel (*17*, *18*). Nevertheless, CGA[1] dissociates from the IP_3R at a near-physiological pH of 7.5 and no longer activates the channel (*17*). However, this is not the case with CGB, which still couples to the IP_3R even at pH 7.5 and activates the channel (*18*). This difference in the IP_3R/Ca^{2+} channel activating properties of CGA and CGB is one of many properties in which these two proteins differ, and is likely to contribute to different Ca^{2+} release responses of a variety of secretory granules (*10*, *11*, *19*−*21*), which contain different kinds of chromogranins at different concentrations (*1*−*7*). Combined with the high-capacity, low-affinity Ca^{2+} storage property, the IP_3R/Ca^{2+} channel activating properties of chromogranins appear to provide the molecular basis for secretory granules to function as a major IP_3-sensitive intracellular Ca^{2+} store of secretory cells (*22*).

Moreover, chromogranins A and B have also been shown to induce de novo secretory granule biogenesis (*23*, *24*), although the granulogenic effect of CGB was 50−60% higher than that of CGA (*24*). Suppression of chromogranin expression in neuroendocrine PC12 cells led to a reduction in the level of intrinsic secretory granules, whereas expression of chromogranins in non-neuroendocrine NIH3T3 and COS-7 cells, which normally do not contain any secretory granules, led to formation of secretory granules (*23*, *24*). Hence, in light of the presence of all three isoforms of IP_3R in secretory granules (*25*), the possibility of the presence of IP_3Rs in the newly formed secretory granules arose. Further, given the major IP_3-sensitive intracellular Ca^{2+} store role of secretory granules (*10*, *11*, *19*−*21*) and that granular Ca^{2+} has been shown to directly control the Ca^{2+} concentrations of the cytoplasm that is immediately adjacent to secretory granules

* To whom correspondence should be addressed. Telephone: 82-32-890-0936. Fax: 82-32-882-0796. E-mail: shyoo@ inha.ac.kr.

§ Present address: Department of Biotechnology, Yonsei University.

[1] Abbreviations: CGA, chromogranin A; CGB, chromogranin B; IP_3R, inositol 1,4,5-trisphosphate receptor; GFP, green fluorescent protein.

10.1021/bi048070w CCC: $30.25
Published on Web 03/29/2005

(*11*), the possibility of a potential contribution of the newly formed secretory granules in the control of IP_3-dependent intracellular Ca^{2+} concentrations became very real.

Therefore, it was of great interest to determine the effect of the presence of secretory granules on the IP_3-induced intracellular Ca^{2+} mobilization in both neuroendocrine and non-neuroendocrine cells. Accordingly, the number of secretory granules and the extent of IP_3-mediated intracellular Ca^{2+} mobilization in these cells were measured, and the relationship between the number of secretory granules present and the magnitude of Ca^{2+} mobilization was investigated. It was hence found that the magnitude of intracellular Ca^{2+} mobilization was closely related to the number of secretory granules present not only in the neuroendocrine PC12 cells but also in the non-neuroendocrine NIH3T3 cells.

EXPERIMENTAL PROCEDURES

Antibodies. Polyclonal anti-rabbit CGA and CGB antibodies were raised against intact bovine CGA and CGB, respectively, and affinity purified on each immobilized purified chromogranin. The specificity of the CGA and CGB antibodies has been confirmed (*26*). IP_3R peptides specific to 10−13 terminal amino acids of type 1 (HPPHMNVNPQQPA), type 2 (SNTPHENHHMPPA), and type 3 (FVDVQNCMSR) were synthesized with a carboxy-terminal cysteine, and anti-rabbit polyclonal antibodies were raised. The polyclonal antibodies were affinity purified on each immobilized peptide following the procedure described previously (*25*), and the specificity of each antibody has been confirmed (*25*). Polyclonal anti-rabbit α-tubulin antibody was obtained from Oncogene.

Construction of Expression Vectors. For the expression vector construction, the cDNAs for CGA and CGB were prepared by polymerase chain reaction (PCR) using bovine cDNA (*27*−*29*) as a template, and the PCR products containing the full coding sequences were subcloned into the EcoRI/XbaI site of the pCI-neo mammalian expression vector (Promega), in which transcription of the cloned gene was under the direction of the constitutively active cytomegalovirus promoter. For chromogranin−green fluorescence protein (GFP) fusion proteins, the reading frames of CGA and CGB without the stop codons were subcloned into the BglII/SalI site of pd2EGFP-N1 vector (Clontech). The PCR products were produced using the following oligodeoxynucleotides: 5′ primer (5′-GCAGATCTGCCTGGAGCGAGCAGTCCA-3′) and 3′ primer (5′-GAGTACTCTCAGCCCCGCCGAAGCTCCTCCA-3′) for the pd2CGA-EGFP construct and 5′ primer (5′-GCAGATCTGGACGAGCGAGGCCAT-3′) and 3′ primer (5′-GAGTACTCTTAGCCCCTTCGGGTACCACTGA-3′) for the pd2CGB-EGFP construct. The circular plasmid cDNAs for transfection were prepared using a Qiagen maxi-preparation kit.

NIH3T3 Cell Culture and Transient Transfection. All culture reagents and powdered media were purchased from GibcoBRL. NIH3T3 cells were maintained in Dulbecco's modified Eagle's medium (DMEM) supplemented with 10% fetal bovine serum. Transient transfection was performed with 70−80% confluent cultures. The cells were transfected with circular plasmid DNAs using LipofecTAMINE-plus transfection reagent (GibcoBRL). Briefly, cells were plated at a density of 5×10^5 cells per well (100 mm in diameter), and were cultured for additional 24 h. Four micrograms of plasmid DNA in 20 μL of LipofecTAMINE was mixed with 750 μL of OPTI-MEM I medium and incubated for 15 min at room temperature. In addition, 30 μL of LipofecTAMINE was mixed with 750 μL of OPTI-MEM I and incubated for 15 min. The mixture was then added to a culture plate containing 5 mL of OPTI-MEM I. The transfection was performed for 3 h at 37 °C. After transfection, the medium was replaced with fresh prewarmed culture medium, and was further incubated for 72 h. In our culture condition, ∼70−80% of NIH3T3 cells were transfected. The pd2EGFP-NI vector was used as an empty vector.

The NIH3T3 cells were also transfected with either IP_3R−siRNAs or IP_3R−siRNAs and pd2CGA-EGFP or pd2CGB-EGFP. The IP_3R-1−siRNA duplex sense and antisense sequences are 5′-CACCACUAUCCAGCACUCAdTdT-3′ and 3′-dTdTGUGGUGAUAGGUCGUGAGU-5′, respectively, and the IP_3R-2−siRNA duplex sense and antisense sequences are 5′-GAAGUUCAGAGACUGCCUCdTdT-3′ and 3′-dTdTCUUCAAGUCUCUGACGGAG-5′, respectively. The IP_3R-3−siRNA duplex sense and antisense sequences are 5′-GCAGAAGAAGGAAGAGAUCdTdT-3′ and 3′-dTdTCGUCUUCUUCCUUCUCUAG-5′, respectively. The two-nucleotide 3′ overhang of 2′-deoxythymidine is indicated as dTdT. The cells were transfected with the siRNAs using the SilencerTM siRNA transfection kit (Ambion). Briefly, approximately 1×10^6 NIH3T3 cells were plated on a culture dish (100 mm in diameter) in DMEM medium supplemented with 10% FBS and were cultured for 24 h before transfection; 1 μg of the appropriate siRNA and 10 μL of siPORT Amine were used per 5×10^5 cells. The transfection was performed for 6 h at 37 °C. After transfection, the medium was replaced with fresh prewarmed DMEM medium, and the mixture was further incubated for 48 h. The transfection was monitored using the Silencer CyTM3 siRNA labeling kit, and the electron microscope and Ca^{2+} measurement experiments were performed using the transfected NIH3T3 cells 48 h after transfection.

PC12 Cell Culture and Transient Transfection of CGA− and CGB−siRNA Duplexes. PC12 cells were maintained in RPMI 1640 (Gibco BRL) medium supplemented with 10% fetal bovine serum. Transient siRNA transfection was performed with 70−80% confluent cultures. The CGA−siRNA duplex sense and antisense sequences are 5′-CAACAACAACACAGCAGCUdTdT-3′ and 3′-dTdTGUUGUUGUUGUGUCGUCGA-5′, respectively, and the CGB−siRNA duplex sense and antisense sequences are 5′-AUGCCCUAUCCAAGUCCAGdTdT-3′ and 3′-dTdTUACGGGAUAGGUUCAGGUC-5′, respectively. The two-nucleotide 3′ overhang of 2′-deoxythymidine is indicated as dTdT. The cells were transfected with the siRNAs using SilencerTM siRNA transfection kit (Ambion). Briefly, approximately $1-2 \times 10^6$ PC12 cells were plated on a collagen type IV (BD Biosciences)-coated culture dish (100 mm in diameter) in RPMI 1640 medium supplemented with 10% FBS and were cultured for 48 h before transfection; 1 μg of the appropriate siRNA and 10 μL of siPORT Amine were used per 5×10^5 cells. Addition of more siRNA did not further reduce the number of secretory granules. The transfection was performed for 6 h at 37 °C. After transfection, the medium was replaced with fresh prewarmed RPMI 1640 medium, and was further incubated for 48 h. The

transfection was monitored using the Silencer CyTM3 siRNA labeling kit, and the electron microscope and Ca^{2+} measurement experiments were performed using the transfected PC12 cells 48 h after transfection.

Extraction of Cellular Proteins and Immunoblot Analysis. To obtain the total cell lysates from the transfected cells, $\sim 3-5 \times 10^6$ cells were washed with ice-cold PBS and lysed in 500 μL of buffer [20 mM Tris-HCl (pH 7.5), 1% Triton X-100, 1 mM EDTA, 1 mM DTT, and 20 μg/mL aprotinin/leupeptin mix]. Then the extracts were incubated for 30 min on ice; the cell debris was removed by centrifugation at 22000*g* for 10 min at 4 °C, and the supernatant was used as the total protein lysate. The proteins (30 μg each) were then resolved by SDS−PAGE, and analyzed by immunoblotting using either the polyclonal anti-rabbit chromogranin and each isoform-specific IP_3R antibody or the monoclonal α-tubulin antibody (Oncogene) and an ECL detection system (Amersham Biosciences).

Determination of $[Ca^{2+}]_i$. NIH3T3 cells transfected with the CGA− or CGB−GFP fusion protein and PC12 cells transfected with the CGA− or CGB−siRNA duplex were stabilized with serum free medium (OPTI-MEM I) for 30 min, and then were loaded with 4 mM fura 2-AM (Molecular Probes) in OPTI-MEM I for 40 min at 37 °C in a 5% CO_2 atmosphere. After incubation, the cells were washed three times with OPTI-MEM I, followed by stabilization with the same medium for 30 min at room temperature. Then, each coverslip containing the cells was mounted on a perfusion chamber, and the NIH3T3 cells that had been successfully transfected with the CGA− or CGB−GFP fusion protein were selected for $[Ca^{2+}]_i$ measurements on the basis of the green fluorescence emission by GFP at 520 nm excitation. Transfection of PC12 cells with siRNAs was monitored using the CGA− or CGB−siRNA duplex labeled with Cy3, and the PC12 cells that emitted red fluorescence at 520 nm excitation were used for $[Ca^{2+}]_i$ measurements. Fura-2 was excited at 340 and 380 nm using a filter wheel controller, and the fluorescence Ca^{2+} images were collected with an Axiovert S 100 fluorescence microscope (Carl Zeiss) at 515 nm. The ratio images were acquired every second and continued with the addition of 100 mM ATP. The changes in fluorescence Ca^{2+} images were analyzed using MetaFluor and MetaMorph (Universal Imaging Corp.). $[Ca^{2+}]_i$ was determined from fura-2 measurements according to the following formula (*30*):

$$[Ca^{2+}]_i = K_d[(R - R_{min})/(R_{max} - R)](F_{f380}/F_{b380})$$

The ratiometric 340/380 value R_{max} and F_{b380} (fluorescence at 380 nm excitation) were obtained after saturating the cells with Ca^{2+} by addition of 10 mM ionomycin and 5 mM Ca^{2+}. R_{min} and F_{f380} were obtained after addition of 10 mM ionomycin and 20 mM EGTA. A K_d of 135 nM (value at 22 °C) was used (*30*).

Electron Microscopy. Cells grown on the culture dish were fixed for 1 h at 4 °C in PBS containing 2% glutaraldehyde, 2% paraformaldehyde, and 3.5% sucrose, but the cells intended for immunogold labeling were fixed in the same solution containing 0.1% glutaraldehyde. The cells were then scraped from the culture dish with a cell scraper and pelleted by centrifugation at 2000*g* for 2 min at 4 °C. The cell pellets were resuspended in warm agar (1% in PBS) and repelleted by centrifugation. After three washes in PBS, the agar-embedded cell pellets were postfixed with 1% osmium tetroxide on ice for 2 h, washed three times, and stained *en block* with 0.5% uranyl acetate, all in PBS. The cell pellets were then embedded in Epon 812 after dehydration in an ethanol series. After collection of the ultrathin sections on Formvar/carbon-coated nickel grids, the grids were stained with uranyl acetate (7 min) and lead citrate (2 min), and were viewed with a Zeiss EM912 electron microscope. The area of the cells was measured, and the number of total dense core granules in the entire measured cell area was counted. The density of granules was determined by dividing the number of secretory granules by the area of the cell.

For immunogold labeling experiments, the ultrathin sections that had been collected on Formvar/carbon-coated nickel grids were floated on drops of freshly prepared 3% sodium metaperiodate for 30 min. The immunogold labeling procedure was modified from that of Spector et al. (*31*) and the manufacturer's recommended protocol (British Biocell International). After being etched and washed, the grids were placed on 50 μL droplets of solution A [phosphate saline solution (pH 8.2) containing 4% normal goat serum, 1% BSA, 0.1% Tween 20, and 0.1% sodium azide] for 30 min. Grids were then incubated for 2 h at room temperature in a humidified chamber on 50 μL droplets of anti-rabbit IP_3R antibodies appropriately diluted in solution B (solution A but with 1% normal goat serum), followed by rinses in solution B. The grids were reacted with 10 nm gold-conjugated goat anti-rabbit IgG diluted in solution A. Controls for the specificity of IP_3R immunogold labeling included (1) omitting the primary antibody and (2) replacing the primary antibody with preimmune serum. After washes in PBS and deionized water, the grids were stained with uranyl acetate (7 min) and lead citrate (2 min), and were viewed with a Zeiss EM912 electron microscope.

RESULTS

IP_3-Induced Intracellular Ca^{2+} Mobilization in NIH3T3 Cells. To determine the effect of chromogranin expression on IP_3-mediated Ca^{2+} release in NIH3T3 cells, the non-neuroendocrine NIH3T3 cells that do not express endogenous CGA or CGB were transfected with either the CGA−EGFP or CGB−EGFP fusion protein, and the expression of CGA and CGB was confirmed (Figure 1A). The IP_3-mediated intracellular Ca^{2+} release of chromogranin-expressing NIH3T3 cells was assessed after application of IP_3-producing agonist ATP. As shown in Figure 2A, IP_3 induced a rapid increase of the intracellular Ca^{2+} concentration, followed by a slow sequestration of the released Ca^{2+} (Figure 2A, trace a). This resulted in an approximately 3.8-fold increase in the intracellular Ca^{2+} concentration over the resting level (Figure 2B). Application of same concentration of ATP to the NIH3T3 cells transfected with EGFP only (empty vector) also induced a rapid increase of the intracellular Ca^{2+} concentration (Figure 2A, trace b), similar to the level shown in the control cells. This resulted in an approximately 3.9-fold increase in the intracellular Ca^{2+} concentration over the resting level (Figure 2B), showing practically no difference between the control cells and the cells transfected with the empty vector.

However, the Ca^{2+} release property of chromogranin-expressing NIH3T3 cells was markedly different (Figure 2A,

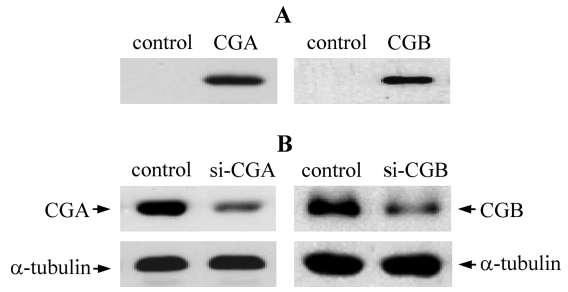

FIGURE 1: Expression and inhibition of chromogranins A and B in transiently transfected NIH3T3 cells and in si-RNA-treated PC12 cells, respectively. (A) The total protein extracts from the NIH3T3 cells transfected with pd2CGA-EGFP (left) or pd2CGB-EGFP (right) were resolved on 10% SDS gels and probed with the anti-CGA (left) or CGB (right) antibody. (B) The expression levels of CGA and CGB in PC12 cells treated with the si-CGA−RNA duplex (left) or the si-CGB−RNA duplex were resolved on 10% SDS gels, and probed with the anti-CGA (left) or CGB (right) antibody. The same blots were reprobed with the α-tubulin antibody after deprobing the first blots to check the amount of protein loaded.

traces c and d). IP_3 released significantly larger amounts of Ca^{2+} from the CGA-expressing NIH3T3 cells than the control cells or the cells transfected with the empty vector (Figure 2A, trace c), inducing a 5.3-fold increase in the intracellular Ca^{2+} concentration over the resting level. This result indicates that approximately 40% more intracellular Ca^{2+} was released in the CGA-transfected cells than in control cells (Figure 2B).

On the other hand, IP_3 induced a rapid and markedly greater increase in intracellular Ca^{2+} concentration from the CGB-expressing cells than any other cells (Figure 2A, trace d). The IP_3-mediated intracellular Ca^{2+} release in the CGB-expressing cells caused an approximately 9.0-fold increase in the intracellular Ca^{2+} concentration over the resting level. This amount of released Ca^{2+} in the CGB-expressing cells is a release of ∼134% more intracellular Ca^{2+} than in the control cells, and is even 68% higher than that of CGA-expressing cells (Figure 2B). Nevertheless, even the high level of released Ca^{2+} was sequestered on a time scale similar to those of other cells, returning to the resting level in ∼100 s (Figure 2A).

Since the expression of chromogranins A and B in NIH3T3 cells induces de novo secretory granule formation (*24*), the increased level of intracellular Ca^{2+} mobilization appeared to result from the IP_3-induced Ca^{2+} releases from the newly formed secretory granules. Consistent with the more effective granulogenic role of CGB, which caused formation of 50−60% more secretory granules than CGA (*24*), the extent of Ca^{2+} mobilization in CGB-transfected NIH3T3 cells was significantly greater than that in the CGA-transfected cells (Figure 2).

Nevertheless, when the expression of the three IP_3R isoforms was suppressed by si-IP_3R−RNA complexes (Figure 3A), the level of IP_3-induced intracellular Ca^{2+} release decreased to 48% of the control (Figure 3B, trace b), indicating a 52% reduction (Figure 3C). On the other hand, the level of IP_3-induced intracellular Ca^{2+} release in the CGA-expressing but si-IP_3R-treated NIH3T3 cells decreased to 70% of the control (Figure 3B, trace c). This level of Ca^{2+} release in the NIH3T3 cells with the newly formed secretory granules was still ∼45% higher than that of the cells treated with si-IP_3R only (Figure 3C), suggesting the contribution

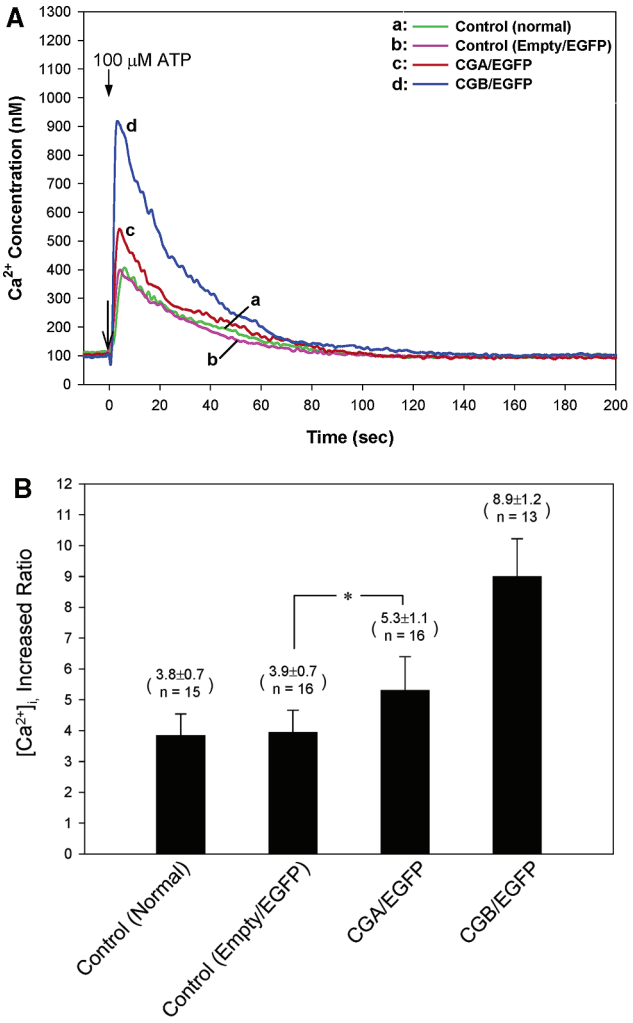

FIGURE 2: Measurement of $[Ca^{2+}]_i$ in chromogranin-transfected NIH3T3 cells. NIH3T3 cells were loaded with fura-2, and the increases in $[Ca^{2+}]_i$ were measured after the cells had been stimulated with 100 μM ATP. (A) The $[Ca^{2+}]_i$ changes in control (a), empty vector-transfected (b), CGA−GFP-transfected (c), and CGB−GFP-transfected (d) NIH3T3 cells are shown. The data shown are representative of similar results repeated 13−16 times. (B) The $[Ca^{2+}]_i$ changes shown in each cell group of panel A are expressed as ratio changes over the respective resting level and are shown in a bar graph (mean ± standard deviation; *n* is the number of experiments). In the paired *t* test, an asterisk indicates $p < 0.001$.

of newly formed secretory granules in the IP_3-mediated Ca^{2+} release. Moreover, the CGB-expressing NIH3T3 cells that contain 50−60% more newly formed secretory granules than the CGA-expressing cells released substantially more Ca^{2+} than the CGA-expressing cells despite the si-IP_3R treatment (Figure 3B, trace d). The IP_3-induced Ca^{2+} release in the CGB-expressing but si-IP_3R-treated cells was similar to that of the control cells (Figure 3B, trace d), and the extent was 110% higher than that in the cells treated with si-IP_3R only (Figure 3C), further suggesting the contribution of secretory granules in the IP_3-induced Ca^{2+} release.

IP_3-Induced Intracellular Ca^{2+} Mobilization in PC12 Cells. To further determine the effect of chromogranin expression on IP_3-mediated Ca^{2+} release in neuroendocrine PC12 cells, PC12 cells that express endogenous CGA and CGB were treated with either the si-CGA− or si-CGB−RNA complex to suppress the expression of either CGA or CGB (Figure 1B), and the IP_3-mediated intracellular Ca^{2+} releases were

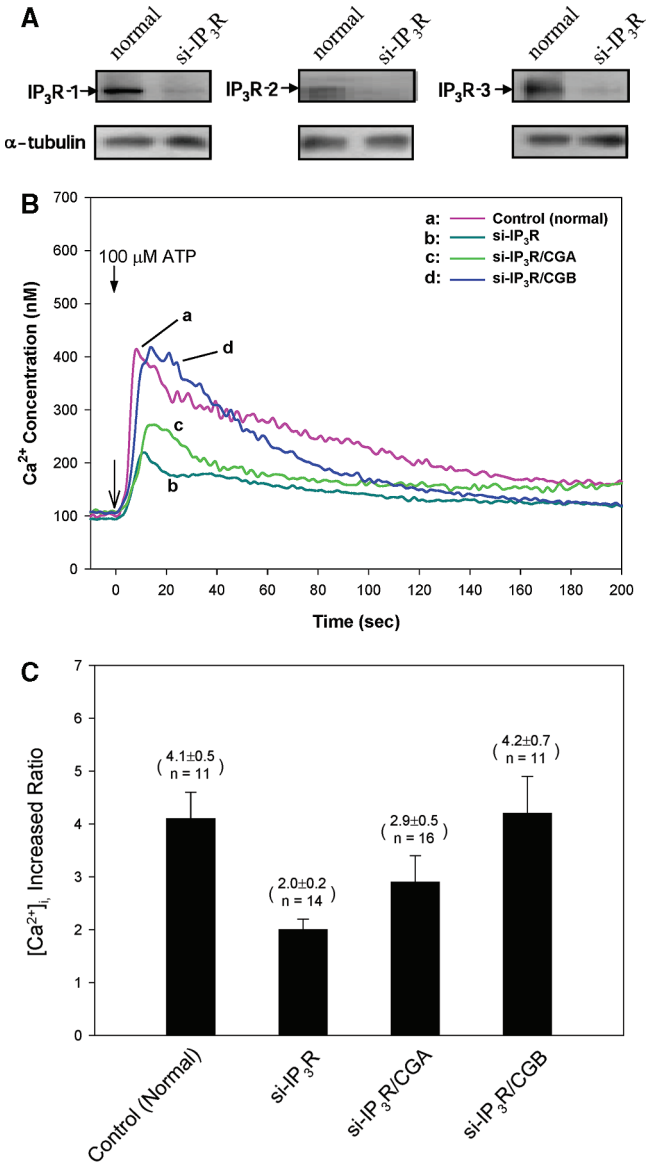

FIGURE 3: Inhibition of IP_3R expression and IP_3-induced Ca^{2+} release in siRNA-treated NIH3T3 cells. (A) The total protein extracts from the NIH3T3 cells treated with si-IP_3Rs were resolved on 7% SDS gels (40 μg/lane) and probed with each IP_3R isoform-specific antibody. The same proteins were resolved on 10% SDS gels (20 μg/lane) and probed with the α-tubulin antibody to check the amount of protein loaded. (B) NIH3T3 cells were loaded with fura-2, and the increases in $[Ca^{2+}]_i$ were measured after the cells had been stimulated with 100 μM ATP. The $[Ca^{2+}]_i$ changes in the following conditions are shown: control (a), si-IP_3R treatment only (b), si-IP_3R treatment, along with CGA−GFP transfection (c), and si-IP_3R treatment, along with CGB−GFP transfection (d). The data shown are representative of similar results recorded 11−16 times. (C) The $[Ca^{2+}]_i$ changes shown in each cell group of panel B are expressed as ratio changes over the respective resting level and are shown in a bar graph (mean ± standard deviation; *n* is the number of experiments).

assessed after application of the IP_3-producing agonist ATP (Figure 4A). Since introduction of the si-CGA- or si-CGB−RNA complex into PC12 cells has been shown to reduce the number of secretory granules in the cells (*24*), the effect of the reduced number of secretory granules on IP_3-mediated Ca^{2+} mobilization was measured in the si-RNA-treated cells.

As shown in Figure 4A, IP_3 induced a rapid and steep increase in the intracellular Ca^{2+} concentration in PC12 cells (Figure 4A, trace a), followed by a slow sequestration of

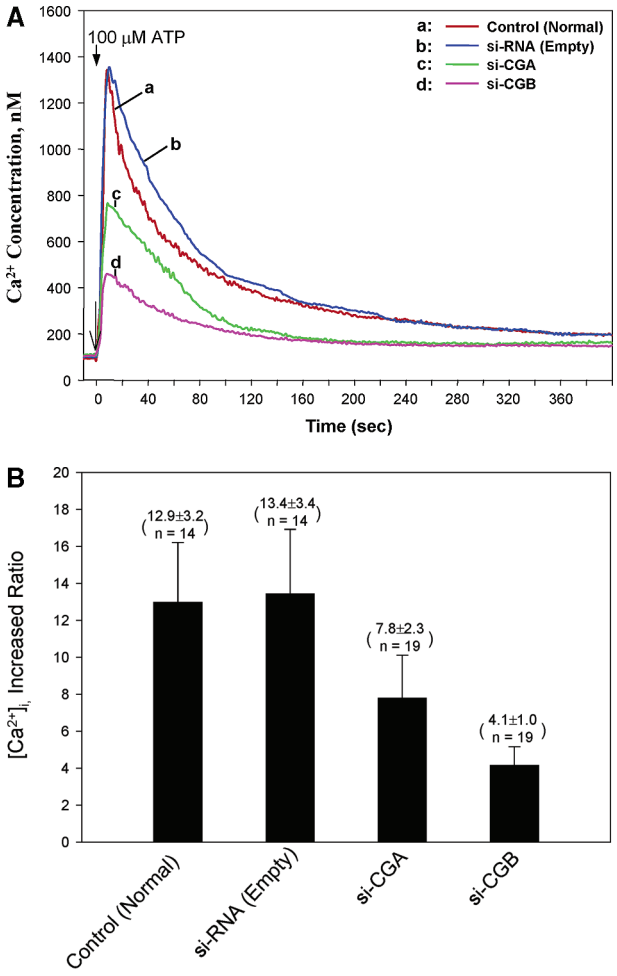

FIGURE 4: Measurement of $[Ca^{2+}]_i$ in PC12 cells treated with the si-CGA− or si-CGB−RNA duplex. PC12 cells were loaded with fura-2, and the increases in $[Ca^{2+}]_i$ were measured after the cells had been stimulated with 100 μM ATP. (A) The $[Ca^{2+}]_i$ changes in control (a), empty si-RNA-treated (b), si-CGA-treated (c), and si-CGB-treated (d) PC12 cells are shown. The data shown are representative of similar results recorded 14−19 times. (B) The $[Ca^{2+}]_i$ changes shown in each cell group of panel A are expressed as ratio changes over the respective resting level and are shown in a bar graph (mean ± standard deviation).

the released Ca^{2+}. Unlike the non-neuroendocrine NIH3T3 cells that do not contain intrinsic secretory granules and released ~3.8−3.9-fold more Ca^{2+} over the resting level (Figures 2 and 3), neuroendocrine PC12 cells that contain intrinsic secretory granules released markedly more Ca^{2+} and resulted in a roughly 13-fold increase in the intracellular Ca^{2+} concentration over the resting level (Figure 4B). Application of the same concentration of ATP to the PC12 cells that had gone through the si-RNA treatment but without the chromogranin si-RNA (empty treatment) also induced a rapid increase in the intracellular Ca^{2+} concentration (Figure 4A, trace b), reaching an approximately 13-fold increase similar to those shown in the control cells (Figure 4B). There was virtually no difference in the levels of intracellular Ca^{2+} mobilized between the control and the empty si-RNA-treated cells.

However, when the PC12 cells that had been treated with the si-CGA−RNA duplex were exposed to the same stimulation, the amount of intracellular Ca^{2+} released was drastically reduced (Figure 4A, trace c), thus reaching an approximately 7.8-fold increase over the resting level (Figure

4B). This amounted to a 40% reduction of the amount of Ca^{2+} released in control cells (Figure 4B). Analogous to the effects of inhibited CGA expression on the IP_3-induced intracellular Ca^{2+} releases, inhibition of CGB expression in PC12 cells also resulted in a marked reduction in the levels of IP_3-mediated intracellular Ca^{2+} release in these cells (Figure 4A, trace d). IP_3 induced an intracellular Ca^{2+} increase of ~4.1-fold over the resting level in the PC12 cells that had been treated with the si-CGB−RNA duplex, indicating a 69% reduction in the amount of Ca^{2+} released in control cells (Figure 4B). Considering that the number of secretory granules in the si-CGB−RNA PC12 cells was reduced by 78% and that of si-CGA-treated cells by 41% (*24*), the amount of intracellular Ca^{2+} mobilized in response to IP_3 appeared to be related to the number of secretory granules present in PC12 cells (Figure 7A).

Immunogold Electron Microscopy of the IP_3Rs in NIH3T3 Cells. In view of the chromogranin-induced secretory granule formation in non-neuroendocrine cells (*23*, *24*) and the increases in the extents of IP_3-induced Ca^{2+} mobilization in these cells (Figures 2 and 3), it was necessary to determine whether the IP_3Rs are also localized in the newly synthesized secretory granules of non-neuroendocrine cells. This possibility was studied using immunogold electron microscopy. As shown in Figures 5 and 6, the IP_3R-labeling immunogold particles were localized in secretory granules of the NIH3T3 cells that had been transfected with either chromogranin A (Figure 5) or chromogranin B (Figure 6). All three isoforms (types 1−3) of the IP_3R were found in both the CGA- and CGB-induced secretory granules, indicating that the secretory granules formed in the NIH3T3 cells also contain all three isoforms of the IP_3R (Figures 5 and 6), as has been the case with secretory granules of neuroendocrine cells (*21*, *22*, *32*).

We compared the degrees of IP_3R expression between the normal NIH3T3 cells and the cells treated with si-IP_3Rs (Tables 1−3). As summarized in Tables 1−3, the number of IP_3R-labeling gold particles per square micrometer of the ER area of normal NIH3T3 cells was 6.4−7.5 while that of the nucleus was 4.5−6.2. However, the si-IP_3R treatment severely reduced the level of expression of all three IP_3R isoforms in the NIH3T3 cells. The number of IP_3R-labeling gold particles per square micrometer of the ER area was 2.4−3.4, while that of the nucleus was 1.4−1.9. When the numbers of nonspecific background IP_3R-labeling gold particles per square micrometer of mitochondria, which are considered to be background, were subtracted from the number of cognate IP_3R isoforms, it became apparent that the si-RNA treatments severely suppressed the expression of all three IP_3R isoforms.

Determination of the relative concentrations of each IP_3R isoform in secretory granules and the ER of the CGA-transfected NIH3T3 cells shows that the ER has 7.3−8.6 IP_3R-labeling gold particles/μm^2 of the ER; secretory granules have 25.3−27.5 IP_3R-labeling gold particles/μm^2, and the nucleus has 5.1−7.9 IP_3R-labeling gold particles/μm^2. When the numbers of IP_3R-labeling gold particles per square micrometer of mitochondria are subtracted from the number of cognate IP_3R isoforms, these results show that the concentration of IP_3R type 1 (IP_3R-1) in secretory granules is ~4.0-fold higher than that of the ER (Table 1) while those of IP_3R type 2 (IP_3R-2) and IP_3R type 3 (IP_3R-3) are ~3.8- and 3.6-fold higher, respectively (Tables 2 and 3).

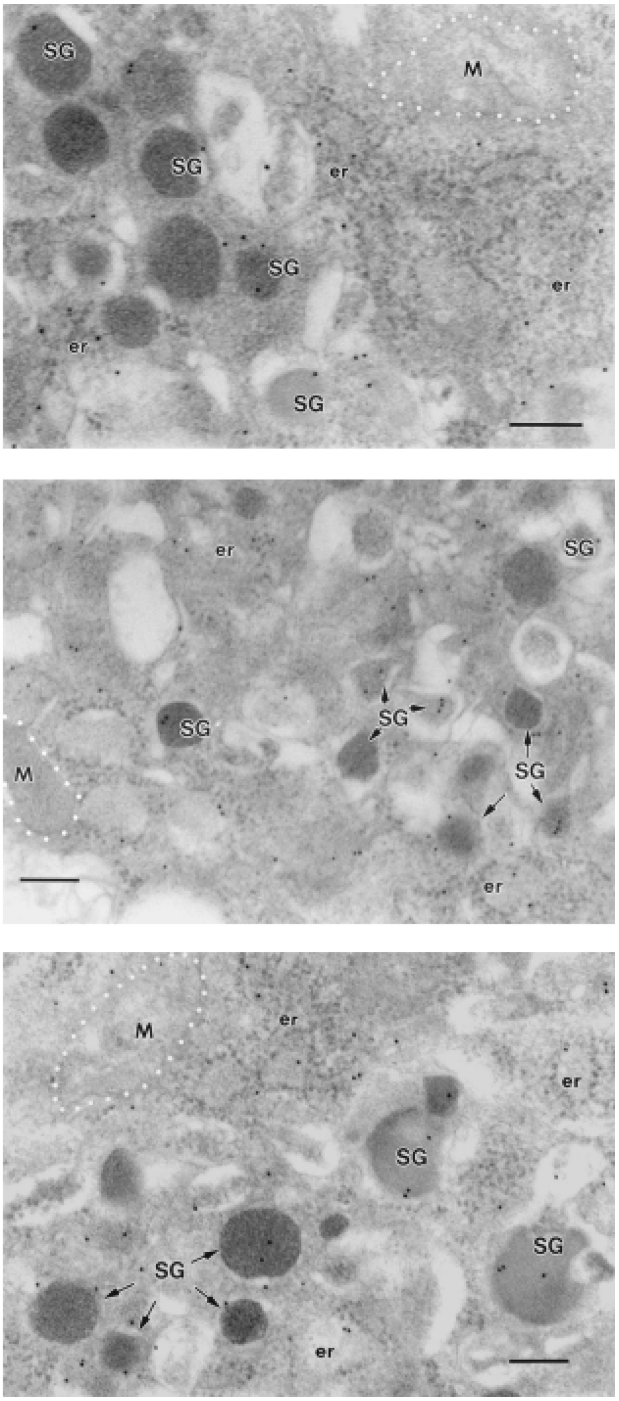

FIGURE 5: Immunogold electron micrographs showing localization of the IP_3Rs in the newly formed secretory granules of CGA-transfected NIH3T3 cells. NIH3T3 cells transfected with CGA were immunolabeled for IP_3R type 1 (A), type 2 (B), and type 3 (C) (15 nm gold) with each affinity-purified isoform-specific IP_3R antibody. The IP_3R-labeling gold particles are localized in the membrane region of the newly formed secretory granules (SG) with some in the endoplasmic reticulum (er), but not in the mitochondria (M). In the control experiments without the primary antibody, no gold particles were seen in secretory granules. The bar is 200 nm.

Similarly, the relative concentrations of each IP_3R isoform in secretory granules and the ER of the CGB-transfected NIH3T3 cells show that the ER has 6.6−8.7 IP_3R-labeling gold particles/μm^2 of the ER; secretory granules have 25.7−27.5 IP_3R-labeling gold particles/μm^2, and the nucleus has 4.8−6.5 IP_3R-labeling gold particles/μm^2. When the numbers

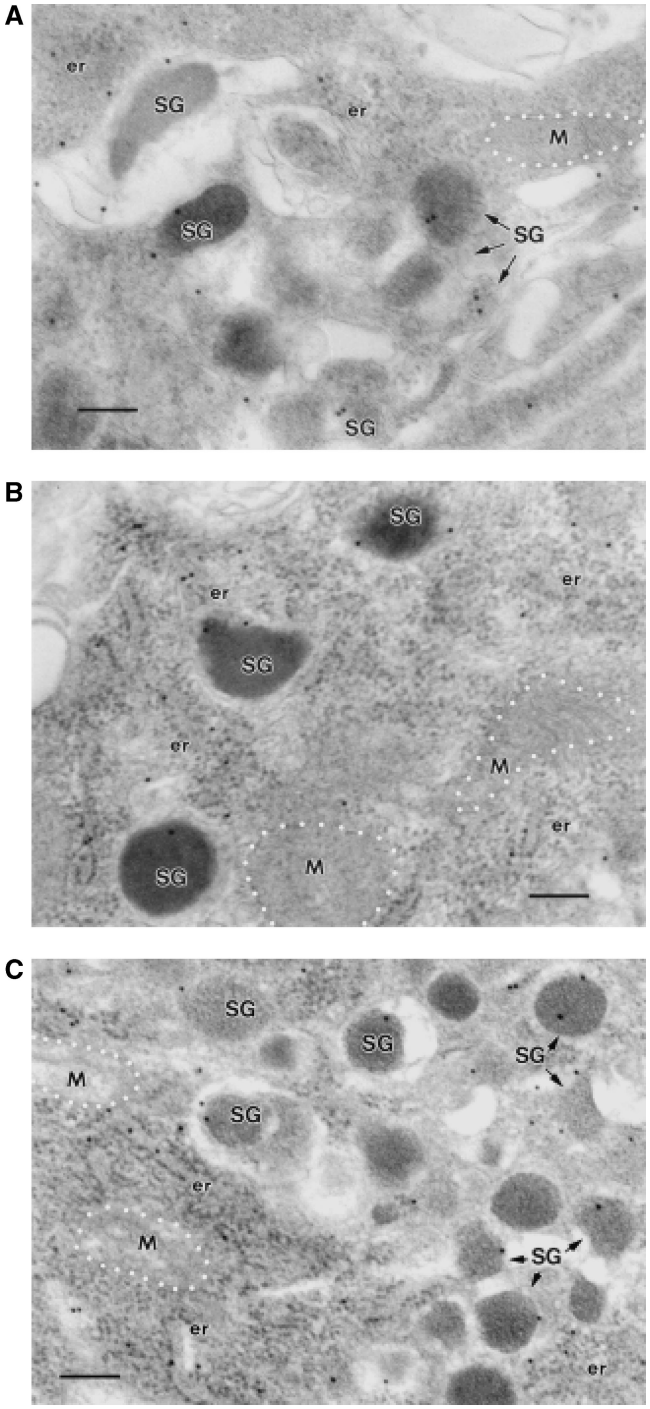

FIGURE 6: Immunogold electron micrographs showing localization of the IP_3Rs in the newly formed secretory granules of CGB-transfected NIH3T3 cells. NIH3T3 cells transfected with CGB were immunolabeled for IP_3R type 1 (A), type 2 (B), and type 3 (C) (15 nm gold) with each affinity-purified isoform-specific IP_3R antibody. The IP_3R-labeling gold particles are localized in the membrane region of the newly formed secretory granules (SG) with some in the endoplasmic reticulum (er), but not in the mitochondria (M). In the control experiments without the primary antibody, no gold particles were seen in secretory granules. The bar is 200 nm.

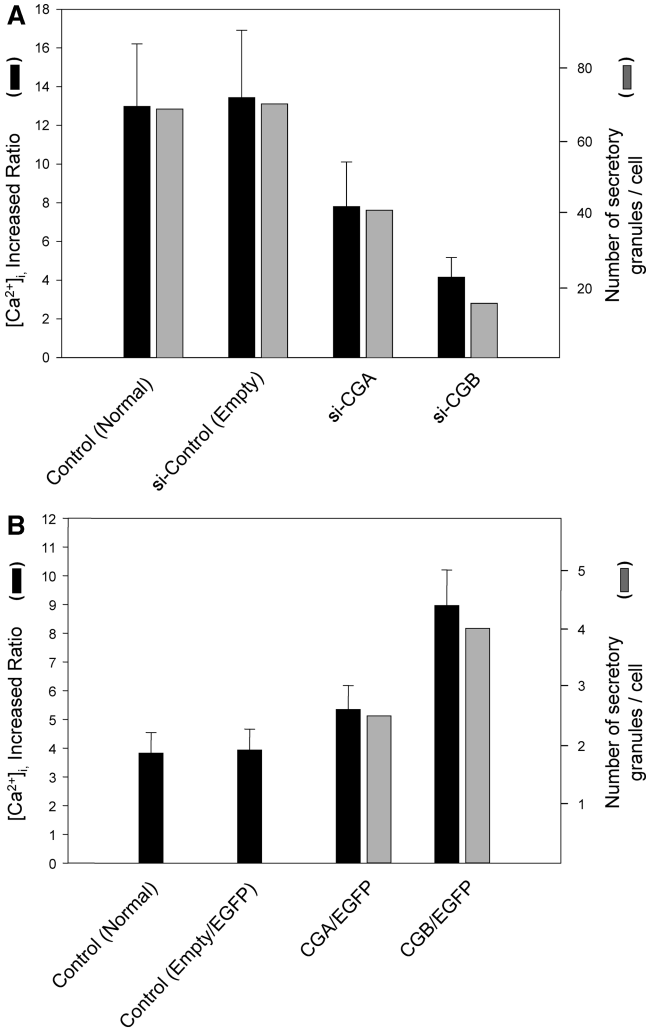

FIGURE 7: Comparison of the increased ratios of $[Ca^{2+}]_i$ with the number of secretory granules in chromogranin-expressing NIH3T3 and PC12 cells. (A) The ratio changes of the $[Ca^{2+}]_i$ in control, empty si-RNA-treated, si-CGA-treated, and si-CGB-treated PC12 cells are shown in comparison with the number of secretory granules per cell. Here, the number of granules per cell indicates the number of granules found in the respective average central section area of a PC12 cell in each group, and the numbers are from published data (Table 2 of ref *24*). (B) The ratio changes of the $[Ca^{2+}]_i$ in control, empty vector-transfected, CGA-EGFP-transfected, and CGB-EGFP-transfected NIH3T3 cells are shown in comparison with the number of secretory granules per cell of CGA- or CGB-expressing NIH3T3 cells. Here, the number of granules per cell indicates the number of granules found in the respective average central section area of an NIH3T3 cell in each group, and the numbers are from published data (Table 1 of ref *24*).

of nonspecific IP_3R-labeling gold particles are subtracted, these results show that the concentration of IP_3R-1 in secretory granules is ~3.8-fold higher than that of the ER (Table 1) while those of IP_3R-2 and IP_3R-3 are ~4.7- and 3.5-fold higher, respectively (Tables 2 and 3). These results are similar to those of CGA-transfected cells, and indicate that the newly formed secretory granules contain similar amounts of IP_3Rs whether they are targeted to the secretory granules by CGA or CGB.

Moreover, these numbers are not that much different from those found in secretory granules of bovine chromaffin cells (*33*); the concentration of IP_3R-1 in secretory granules of bovine chromaffin cells was 4.4-fold higher than that of the ER, while those of IP_3R-2 and IP_3R-3 were 3.6- and 3.7-fold higher, respectively, thus suggesting that the relative concentrations of the IP_3Rs in secretory granules do not vary much whether the secretory granules are endogenous or induced. Comparison of the relative concentrations of the IP_3R isoforms expressed in both the ER and nucleus of CGA- or CGB-transfected and nontransfected NIH3T3 cells did not show significant differences. The ER/nucleus concentration

Table 1: Distribution of the IP_3R Type 1-Labeled Gold Particles in NIH3T3 Cells[a]

	normal[b]		si-IP_3R-1[c]		CGA[b]		si-IP_3R-1 and CGA[c]		CGB[b]		si-IP_3R-1 and CGB[c]	
	no. of gold particles/ area viewed (μm^2)	no. of gold particles/ μm^2	no. of gold particles/ area viewed (μm^2)	no. of gold particles/ μm^2	no. of gold particles/ area viewed (μm^2)	no. of gold particles/ μm^2	no. of gold particles/ area viewed (μm^2)	no. of gold particles/ μm^2	no. of gold particles/ area viewed (μm^2)	no. of gold particles/ μm^2	no. of gold particles/ area viewed (μm^2)	no. of gold particles/ μm^2
endoplasmic reticulum	76/10.2	7.5	19/5.6	3.4	373/51.1	7.3	34/7.3	4.6	442/61.6	7.2	29/5.9	4.9
secretory granules	NA	NA	NA	NA	165/6.3	26.2	24/2.0	12.0	167/6.5	25.7	31/3.5	8.9
nucleus	106/23.5	4.5	33/17.7	1.9	157/30.8	5.1	19/8.3	2.3	245/51.0	4.8	10/4.2	2.4
mitochondria	6/8.2	0.7	1/3.2	0.3	4/4.1	1.0	1/1.1	0.9	2/3.0	0.7	3/2.5	1.2

[a] The values are from normal (untreated control), si-RNA-treated (si-IP_3R-1), CGA-transfected (CGA), CGB-transfected (CGB), CGA-transfected but si-RNA-treated (si-IP_3R and CGA), or CGB-transfected but si-RNA-treated (si-IP_3R and CGB) NIH3T3 cells. [b] Fifteen images from five different tissue preparations were used. [c] Seven images from three different tissue preparations were used.

Table 2: Distribution of the IP_3R Type 2-Labeled Gold Particles in NIH3T3 Cells[a]

	normal[b]		si-IP_3R-2[c]		CGA[b]		si-IP_3R-2 and CGA[c]		CGB[b]		si-IP_3R-2 and CGB[c]	
	no. of gold particles/ area viewed (μm^2)	no. of gold particles/ μm^2	no. of gold particles/ area viewed (μm^2)	no. of gold particles/ μm^2	no. of gold particles/ area viewed (μm^2)	no. of gold particles/ μm^2	no. of gold particles/ area viewed (μm^2)	no. of gold particles/ μm^2	no. of gold particles/ area viewed (μm^2)	no. of gold particles/ μm^2	no. of gold particles/ area viewed (μm^2)	no. of gold particles/ μm^2
endoplasmic reticulum	46/7.2	6.4	17/6.9	2.5	407/54.8	7.4	30/12.3	2.4	414/62.3	6.6	19/7.2	2.6
secretory granules	NA	NA	NA	NA	134/5.3	25.3	23/2.1	10.9	180/6.8	26.5	29/4.7	6.2
nucleus	144/23.3	6.2	26/18.1	1.4	303/45.3	6.7	8/3.2	2.5	550/84.6	6.5	21/6.0	3.5
mitochondria	5/7.1	0.7	1/4.9	0.2	5/4.4	1.1	3/2.9	1.0	3/2.6	1.2	3/3.0	1.0

[a] The values are from normal (untreated control), si-RNA-treated (si-IP_3R-2), CGA-transfected (CGA), CGB-transfected (CGB), CGA-transfected but si-RNA-treated (si-IP_3R and CGA), or CGB-transfected but si-RNA-treated (si-IP_3R and CGB) NIH3T3 cells. [b] Fifteen images from five different tissue preparations were used. [c] Seven images from three different tissue preparations were used.

Table 3: Distribution of the IP_3R Type 3-Labeled Gold Particles in NIH3T3 Cells[a]

	normal[b]		si-IP_3R-3[c]		CGA[b]		si-IP_3R-3 and CGA[c]		CGB[b]		si-IP_3R-3 and CGB[c]	
	no. of gold particles/ area viewed (μm^2)	no. of gold particles/ μm^2	no. of gold particles/ area viewed (μm^2)	no. of gold particles/ μm^2	no. of gold particles/ area viewed (μm^2)	no. of gold particles/ μm^2	no. of gold particles/ area viewed (μm^2)	no. of gold particles/ μm^2	no. of gold particles/ area viewed (μm^2)	no. of gold particles/ μm^2	no. of gold particles/ area viewed (μm^2)	no. of gold particles/ μm^2
endoplasmic reticulum	62/8.0	7.8	13/5.5	2.4	550/63.7	8.6	20/6.0	3.3	455/52.2	8.7	26/7.5	3.5
secretory granules	NA	NA	NA	NA	234/8.5	27.5	17/1.9	8.9	206/7.5	27.5	41/5.1	8.0
nucleus	99/17.1	5.8	28/19.1	1.5	486/61.6	7.9	10/3.8	2.6	196/34.5	5.7	15/6.4	2.3
mitochondria	3/6.2	0.5	2/5	0.4	6/4.8	1.3	1/1.1	0.9	3/2.7	1.1	1/0.9	1.1

[a] The values are from normal (untreated control), si-RNA-treated (si-IP_3R-3), CGA-transfected (CGA), CGB-transfected (CGB), CGA-transfected but si-RNA-treated (si-IP_3R and CGA), or CGB-transfected but si-RNA-treated (si-IP_3R and CGB) NIH3T3 cells. [b] Fifteen images from five different tissue preparations were used. [c] Seven images from three different tissue preparations were used.

ratios of each IP_3R isoform in the normal NIH3T3 cells ranged from 1.0 to 1.8, while that of CGA- or CGB-transfected NIH3T3 cells ranged from 1.0 to 1.7 (Tables 1−3), exhibiting little difference between the two cell groups.

Identical experiments with the CGA- or CGB-transfected but si-IP_3R-treated NIH3T3 cells showed that the number of IP_3R-labeling gold particles per square micrometer of the ER and nucleus was 2.4−4.9 or 2.3−3.5, respectively, while that of secretory granules was 6.2−12.0 (Tables 1−3), showing markedly reduced levels of the IP_3R isoforms in the si-IP_3R-treated cells. When the nonspecific background IP_3R-labeling gold particles were subtracted, it became evident that the expression of all three IP_3R isoforms is severely reduced even in the si-IP_3R-treated but chromogranin-expressing NIH3T3 cells. Despite the suppression of the IP_3R expression in the si-IP_3R-treated but chromogranin-expressing NIH3T3 cells, the number of newly formed secretory granules in these cells did not decrease compared to that of the control cells, i.e., chromogranin-expressing but not si-IP_3R-treated cells (not shown).

Correlation between the Number of Secretory Granules and Intracellular Ca^{2+} Release. To determine the level of

correlation between the number of secretory granules present in each cell and the amount of intracellular Ca^{2+} released in response to IP_3, the number of secretory granules present in chromogranin-transfected NIH3T3 cells and the siRNA-treated PC12 cells was compared with the amount of Ca^{2+} released in each cell (Figure 7). As has been shown previously, suppression of CGA and CGB expression in PC12 cells resulted in the reduction of the number of endogenous secretory granules by 41 and 78%, respectively (*24*). Like the reduction of the number of secretory granules, the extents of IP_3-mediated Ca^{2+} release also decreased by 40 and 69% in the si-CGA− and si-CGB−RNA-transfected PC12 cells, respectively (Figure 7A). There appeared to be a close correlation between the number of secretory granules and the extent of IP_3-induced intracellular Ca^{2+} mobilization in neuroendocrine PC12 cells.

Since there are no endogenous secretory granules in non-neuroendocrine NIH3T3 cells, the extent of IP_3-induced Ca^{2+} release in normal NIH3T3 cells could not be directly correlated with the number of secretory granules. However, the effect of CGA or CGB expression on the IP_3-mediated intracellular Ca^{2+} mobilization was evident; the magnitude of IP_3-induced intracellular Ca^{2+} releases in CGA- and CGB-expressing NIH3T3 cells was 40 and 134% higher, respectively, compared to the control cells or the cells transfected with the empty vector (Figure 2B). In view of the presence of secretory granules in both CGA- and CGB-expressing NIH3T3 cells, it was therefore possible to compare the number of secretory granules formed in the cytoplasm with the extent of IP_3-induced Ca^{2+} mobilization in these cells (Figure 7B).

As has been reported previously (*24*), the number of secretory granules in CGB-expressing NIH3T3 cells was 50−60% higher than that of CGA-expressing cells. Likewise, the extents of IP_3-induced Ca^{2+} release in CGB-expressing cells were ∼68% higher than those of CGA-expressing cells, implying a relationship between the number of secretory granules and the magnitude of IP_3-mediated Ca^{2+} releases in NIH3T3 cells (Figure 7B).

DISCUSSION

These results show that IP_3 mobilizes far larger amounts of intracellular Ca^{2+} in chromogranin-expressing cells than in chromogranin-suppressed or nonexpressing cells. Chromogranins are normally expressed in secretory cells (neurons, endo/exocrine cells, and neuroendocrine cells), and non-neuroendocrine cells such as NIH3T3 cells do not express chromogranins. Nevertheless, IP_3 mobilized significantly larger amounts of intracellular Ca^{2+} in chromogranin-expressing NIH3T3 cells than in control cells (Figure 2). In particular, CGB had a more profound effect on IP_3-mediated intracellular Ca^{2+} mobilization than CGA.

The extent of IP_3-mediated Ca^{2+} release in CGA-expressing NIH3T3 cells was ∼40% higher than that of the control cells (Figure 2). Like the CGA-expressing cells, the CGB-expressing NIH3T3 cells also released markedly larger amounts of Ca^{2+} in response to the same stimulation. In the case of CGB-expressing NIH3T3 cells, the extent of IP_3-mediated Ca^{2+} release was more than 2-fold higher than that of control cells, and was even 68% higher than that of CGA-expressing cells (Figure 2), suggesting a greater effect of CGB in IP_3-mediated intracellular Ca^{2+} mobilization. Since expression of either CGA or CGB in non-neuroendocrine NIH3T3 and COS-7 cells has previously been demonstrated to induce de novo secretory granule formation in these cells (*23*, *24*), these results indicate that the IP_3-mediated intracellular Ca^{2+} mobilization in these cells is directly affected by the expression of the chromogranins.

On the other hand, suppression of chromogranin expression in neuroendocrine PC12 cells had the opposite effect. By suppressing the expression of intrinsic CGA or CGB in PC12 cells by treating PC12 cells with si-CGA− or si-CGB−RNA (Figure 1B), the number of secretory granules in si-CGA-treated PC12 cells decreased by 41% while that in si-CGB-treated cells decreased by 78% (*24*). This decrease in the number of secretory granules in PC12 cells was shown in this study to result in the decrease in the amount of IP_3-induced intracellular Ca^{2+} release (Figure 4). As shown in Figure 4, stimulation of control PC12 cells with 100 μM ATP caused an ∼13-fold increase in the intracellular Ca^{2+} concentration over the resting level. Similar results were also observed in the PC12 cells treated with the si-RNA reagents but without the CGA or CGB RNA (empty). However, stimulation of the si-CGA-treated PC12 cells with the same agonist caused an ∼7.8-fold increase in the intracellular Ca^{2+} concentration over the resting level, indicating a 40% reduction in the extent of the released Ca^{2+} in these cells compared to the control cells. Moreover, IP_3 caused an only 4.1-fold increase in the intracellular Ca^{2+} concentration in the si-CGB-treated PC12 cells, indicating a 69% reduction in the amount of intracellular Ca^{2+} released.

Since the newly formed secretory granules cannot function as IP_3-sensitive intracellular Ca^{2+} stores in the absence of the IP_3Rs, the presence of the IP_3Rs in secretory granules of chromogranin-expressing NIH3T3 cells agrees well with the increase in the extent of IP_3-induced intracellular Ca^{2+} releases in these secretory granule-containing cells. Furthermore, the close correlation between the number of secretory granules and the magnitude of IP_3-induced Ca^{2+} release highlights the importance of IP_3-induced Ca^{2+} release from secretory granules in the IP_3-dependent intracellular Ca^{2+} mobilization in the cell. Nevertheless, the fact that the IP_3R concentration ratios of ER/nucleus remain similar between the chromogranin-transfected and nontransfected NIH3T3 cells suggests that the IP_3Rs expressed in the ER and nucleus of NIH3T3 cells are not affected by the formation of secretory granules.

Nonetheless, this should not be confused with the de novo production of the IP_3Rs in the newly formed secretory granules of chromogranin-expressing NIH3T3 cells. The IP_3R concentrations in the newly formed secretory granules of NIH3T3 cells were shown to be 3.5−4.7-fold higher than those of the ER (Tables 1−3), which are similar to the levels shown in secretory granules and the ER of neuroendocrine chromaffin cells (Table 1 of ref *33*). In light of the observation that the expression of intrinsic IP_3Rs in the ER and nucleus of NIH3T3 cells does not change regardless of the chromogranin expression, these results indicate that the chromogranin expression induced production of all three isoforms of the IP_3Rs that were targeted to the newly formed secretory granules of NIH3T3 cells. The 3.5−4.7-fold higher concentrations of the IP_3Rs in secretory granules, compared

to those of the ER, make it clear why chromogranin expression enhances the IP_3-dependent Ca^{2+} storage and release capabilities of the cells in which they are expressed. Moreover, these results also indicate that the higher magnitude of IP_3-dependent Ca^{2+} release in CGB-expressing, than CGA-expressing, NIH3T3 cells is not because of the higher concentrations of the IP_3Rs in the newly formed secretory granules of CGB-expressing cells but because of the larger number of secretory granules formed in CGB-expressing cells, which is 50−60% higher, than in the CGA-expressing cells (*24*).

The contribution of the newly formed secretory granules to the IP_3-induced intracellular Ca^{2+} release in the chromogranin-expressing NIH3T3 cells is also manifested by the suppression of IP_3R expression. As shown in Figure 3 and Tables 1−3, suppression of the IP_3R expression by si-IP_3R−RNA duplexes specific to all three IP_3R isoforms in NIH3T3 cells resulted in the reduction in the extents of IP_3-induced Ca^{2+} release (Figure 3B). Even in this case, the CGA- and CGB-expressing NIH3T3 cells released 45 and 110%, respectively, more Ca^{2+} than the cells that were devoid of the chromogranin expression, demonstrating the contribution of the newly formed secretory granules to the IP_3-induced intracellular Ca^{2+} release. Nevertheless, although the number of newly formed secretory granules in the chromogranin-expressing but si-IP_3R-treated NIH3T3 cells remained unchanged, the magnitude of IP_3-induced intracellular Ca^{2+} release in these cells was substantially lower than in those cells that were not treated with the si-IP_3R−RNA complexes (Figure 3B). In view of the inhibition of the IP_3R expression in the si-IP_3R-treated cells (Figure 3A and Tables 1−3), the reduction in the magnitude of IP_3-induced intracellular Ca^{2+} release in the chromogranin-expressing but si-IP_3R-treated NIH3T3 cells indicates the IP_3-mediated Ca^{2+} release through the IP_3R/Ca^{2+} channels of the newly formed secretory granules.

The significantly higher magnitude of IP_3-induced Ca^{2+} mobilization in PC12 cells, reaching ~1.35 μM (Figure 4A), compared to that of NIH3T3 cells, reaching ~0.4 μM (Figure 2A), appeared to reflect the abundance of intrinsic secretory granules in PC12 cells. Even in the case of chromogranin-expressing NIH3T3 cells, the number of secretory granules formed per NIH3T3 cell was markedly lower than that of PC12 cells (*24*). So despite the significantly increased magnitude of IP_3-induced Ca^{2+} mobilization in the secretory granule-containing NIH3T3 cells (Figure 2), the overall ability to mobilize intracellular Ca^{2+} in the NIH3T3 cells was far short of the similar ability of PC12 cells (Figure 4), which contain a significantly larger number of secretory granules (*24*).

In addition to the granulogenic roles, it has recently been shown that CGA and CGB activate the IP_3R/Ca^{2+} channels, increasing the open probability and the mean open time of the channel (*17, 18*). Chromogranin A couples to the IP_3R at an intragranular pH of 5.5 and increases the open probability of the IP_3R/Ca^{2+} channel by 9-fold and the mean open time by 12-fold (*17*). But when CGA is dissociated from the IP_3R/Ca^{2+} channel at a near-physiological pH of 7.5, the channel activity returns to a control level, underscoring the IP_3R/Ca^{2+} channel-activating role of CGA. Like chromogranin A, chromogranin B also couples to the IP_3R at pH 5.5 and increases the open probability of the IP_3R/Ca^{2+} channel by 16-fold and the mean open time by 42-fold (*18*). However, unlike CGA, which dissociates from the IP_3R at pH 7.5, CGB stays bound to the IP_3R even at pH 7.5 (*32*) and activates the IP_3R/Ca^{2+} channel, increasing the open probability of the channel by 8-fold and the mean open time by 23-fold. Coupling of the equimolar mixture of CGA and CGB to the IP_3R/Ca^{2+} channel also exhibited IP_3R/Ca^{2+} channel-activating effects similar to those of CGB alone (*18*). Since the equimolar mixture of CGA and CGB forms a CGA−CGB heterodimer at a near-physiological pH of 7.5 and a CGA_2−CGB_2 heterotetramer at an intragranular pH of 5.5 (*34*), the channel-activating effect of CGA−CGB mixture is presumed to result from the interaction of CGB with the IP_3R at both pH 5.5 and 7.5 (*32*).

Indeed, interaction of CGB with the IP_3Rs of the ER at a pH of 7.4 has been shown to be essential in controlling the IP_3-dependent release of Ca^{2+} from the ER (*35*). Using neuronally differentiated PC12 cells, Ehrlich and colleagues (*35*) have demonstrated that IP_3-dependent Ca^{2+} release from the ER is controlled primarily by the functional coupling between chromogranins and the IP_3Rs in the ER. In light of formation of the CGA−CGB heterodimer at a near-physiological pH of 7.5 (*34*), CGA appeared to participate in the control of the IP_3Rs even in the ER. These results indicated that the coupling between chromogranins and the IP_3R/Ca^{2+} channels is an essential component in controlling the IP_3-dependent intracellular Ca^{2+} concentrations in the cell (*35*), and further suggested that the relative concentrations of chromogranins and the IP_3Rs in subcellular organelles determine the IP_3-induced Ca^{2+} release property of the cell.

Chromogranins A and B that are coupled to the IP_3R are known to change the conformation of the IP_3R to a more ordered form, making it more conducive to IP_3 binding and release of Ca^{2+} (*16, 18*). Combined with the high-capacity Ca^{2+} storage properties of chromogranins A and B, binding 50−90 Ca^{2+}/mol (*14, 15*), the presence of IP_3R/Ca^{2+} channel-coupled chromogranins in secretory granules will greatly increase the amount of Ca^{2+} that can be released from secretory granules. It is therefore likely that a given concentration of IP_3 will induce release of more intracellular Ca^{2+} in the cells that contain more secretory granules. This appears to be the case not only in PC12 cells that contain intrinsic secretory granules and chromogranins A and B (*36, 37*) but also in chromogranin-transfected non-neuroendocrine NIH3T3 cells that contain chromogranins inside the newly synthesized secretory granules (*24*).

Targeting of the IP_3R to the chromogranin-induced secretory granules is a first demonstration of chromogranin-directed targeting of an integral membrane protein to newly formed secretory granules. Since both CGA and CGB have been known to directly interact with the IP_3R (*32*), localization of the IP_3Rs in secretory granules, be they endogenous or induced, appears to result from direct interaction between chromogranins and the IP_3R. Hence, this cotargeting of chromogranins and the IP_3R to secretory granules underscores the granulogenic roles CGA and CGB play in selective segregation and targeting of secretory granule membrane proteins, including the IP_3R, to secretory granules during secretory granule biogenesis.

The granulogenic role of chromogranins A and B is now further extended to other regulated secretory proteins such as secretogranin II and hormone precursors pro-vasopressin,

pro-oxytocin, and pro-opiomelanocortin (*38*). Nevertheless, the granulogenic effect of CGB and SgII was far greater than that of the hormone precursors; CGB and secretogranin II induced secretory granule formation in all the transfected cells, whereas the hormone precursors did the same in only a limited number of transfected cells (*38*).

REFERENCES

1. Winkler, H., and Fischer-Colbrie, R. (1992) The chromogranins A and B: The first 25 years and future perspectives, *Neuroscience 49*, 497−528.
2. Helle, K. B. (2000) The chromogranins: Historical perspectives, *Adv. Exp. Med. Biol. 482*, 3−20.
3. Aunis, D., and Metz-Boutigue, M. H. (2000) Chromogranins: Current Concepts. Structural and functional aspects, *Adv. Exp. Med. Biol. 482*, 21−38.
4. Taupenot, L., Harper, K. L., and O'Connor, D. T. (2003) The chromogranin-secretogranin family, *N. Engl. J. Med. 348*, 1134−1149.
5. Huttner, W. B., Gerdes, H.-H., and Rosa, P. (1991) in *Markers for Neural and Endocrine Cells, Molecular and Cell Biology, Diagnostic Application* (Gratzl, M., and Langley, K., Eds.) pp 93−131, VCH, Weinheim, Germany.
6. Winkler, H., and Westhead, E. (1980) The molecular organization of adrenal chromaffin granules, *Neuroscience 5*, 1803−1823.
7. Hutton, J. C. (1989) The insulin secretory granule, *Diabetologia 32*, 271−281.
8. Haigh, J. R., Parris, R., and Phillips, J. H. (1989) Free concentrations of sodium, potassium and calcium in chromaffin granules, *Biochem. J. 259*, 485−491.
9. Bulenda, D., and Gratzl, M. (1985) Matrix free Ca^{2+} in isolated chromaffin vesicles, *Biochemistry 24*, 7760−7765.
10. Gerasimenko, O. V., Gerasimenko, J. V., Belan, P. V., and Petersen, O. H. (1996) Inositol trisphosphate and cyclic ADP-ribose-mediated release of Ca^{2+} from single isolated pancreatic zymogen granules, *Cell 84*, 473−480.
11. Nguyen, T., Chin, W.-C., and Verdugo, P. (1998) Role of Ca^{2+}/K^{+} ion exchange in intracellular storage and release of Ca^{2+}, *Nature 395*, 908−912.
12. Grinstein, S., Furuya, W., VanderMeulen, J., and Hancock, R. G. V. (1983) The total and free concentrations of Ca^{2+} and Mg^{2+} inside platelet secretory granules, *J. Biol. Chem. 258*, 14774−14777.
13. Quesada, I., Chin, W.-C., Steed, J., Campos-Bedolla, P., and Verdugo, P. (2001) Mouse mast cell secretory granules can function as intracellular ionic oscillators, *Biophys. J. 80*, 2133−2139.
14. Yoo, S. H., and Albanesi, J. P. (1991) High-capacity, low-affinity Ca^{2+} binding of chromogranin A: Relationship between the pH-induced conformational change and Ca^{2+} binding property, *J. Biol. Chem. 266*, 7740−7745.
15. Yoo, S. H., Oh, Y. S., Kang, M. K., Huh, Y. H., So, S. H., Park, H. S., and Park, H. Y. (2001) Localization of Three Subtypes of the Inositol 1,4,5-Trisphosphate Receptor/Ca^{2+} Channel in the Secretory Granules and Coupling with the Ca^{2+} Storage Proteins Chromogranins A and B, *J. Biol. Chem. 276*, 45806−45812.
16. Yoo, S. H., and Jeon, C. J. (2000) Inositol 1,4,5-Trisphosphate Receptor/Ca^{2+} Channel Modulatory Role of Chromogranin A, a Ca^{2+} Storage Protein of Secretory Granules, *J. Biol. Chem. 275*, 15067−15073.
17. Thrower, E. C., Park, H. Y., So, S. H., Yoo, S. H., and Ehrlich, B. E. (2002) Activation of the Inositol 1,4,5-Trisphosphate Receptor by the Ca^{2+} Storage Protein Chromogranin A, *J. Biol. Chem. 277*, 15801−15806.
18. Thrower, E. C., Choe, C. U., So, S. H., Jeon, S. H., Ehrlich, B. E., and Yoo, S. H. (2003) A Functional Interaction between Chromogranin B and the Inositol 1,4,5-Trisphosphate Receptor/Ca^{2+} Channel, *J. Biol. Chem. 278*, 49699−49706.
19. Yoo, S. H., and Albanesi, J. P. (1990) Inositol 1,4,5-Trisphosphate-triggered Ca^{2+} Release from Bovine Adrenal Medullary Secretory Vesicles, *J. Biol. Chem. 265*, 13446−13448.
20. Blondel, O., Bell, G. I., Moody, M., Miller, R. J., and Gibbons, S. J. (1994) Creation of an inositol 1,4,5-trisphosphate-sensitive Ca^{2+} store in secretory granules of insulin-producing cells, *J. Biol. Chem. 269*, 27167−27170.
21. Srivastava, M., Atwater, I., Glasman, M., Leighton, X., Goping, G., Caohuy, H., Miller, G., Pichel, J., Westphal, H., Mears, D., Rojas, E., and Pollard, H. B. (1999) Defects in inositol 1,4,5-trisphosphate receptor expression, Ca^{2+} signaling, and insulin secretion in the anx7(+/−) knockout mouse, *Proc. Natl. Acad. Sci. U.S.A. 96*, 13783−13788.
22. Yoo, S. H. (2000) Coupling of the Inositol 1,4,5-Trisphosphate Receptor/Ca^{2+} Channel and Ca^{2+} Storage Proteins Chromogranins A and B in Secretory Granules, *Trends Neurosci. 23*, 424−428.
23. Kim, T., Tao-Cheng, J.-H., Eiden, L. E., and Loh, Y. P. (2001) Chromogranin A, an on/off switch controlling dense-core secretory granule biogenesis, *Cell 106*, 499−509.
24. Huh, Y. H., Jeon, S. H., and Yoo, S. H. (2003) Chromogranin B-induced Secretory Granule Biogenesis: Comparison with the Similar Role of Chromogranin A, *J. Biol. Chem. 278*, 40581−40589.
25. Yoo, S. H., Oh, Y. S., Kang, M. K., Huh, Y. H., So, S. H., Park, H. S., and Park, H. Y. (2001) Localization of Three Subtypes of the Inositol 1,4,5-Trisphosphate Receptor/Ca^{2+} Channel in the Secretory Granules and Coupling with the Ca^{2+} Storage Proteins Chromogranins A and B, *J. Biol. Chem. 276*, 45806−45812.
26. Park, H. Y., So, S. H., Lee, W. B., You, S. H., Kang, M. K., and Yoo, S. H. (2002) Purification, pH-dependent Conformational Change, Aggregation, and Secretory Granule Membrane Binding Property of Secretogranin II (Chromogranin C), *Biochemistry 41*, 1259−1266.
27. Iacangelo, A., Affolter, H.-U., Eiden, L. E., Herbert, E., and Grimes, M. (1986) Bovine chromogranin A sequence and distribution of its messenger RNA in endocrine tissues, *Nature 323*, 82−86.
28. Benedum, U. M., Baeuerle, P. A., Konecki, D. S., Frank, R., Powell, J., Mallet, J., and Huttner, W. B. (1986) The primary structure of bovine chromogranin A: A representative of a class of acidic secretory proteins common to a variety of peptidergic cells, *EMBO J. 5*, 1495−1502.
29. Bauer, J. W., and Fischer-Colbrie, R. (1991) Primary structure of bovine chromogranin B deduced from cDNA sequence, *Biochim. Biophys. Acta 1089*, 124−126.
30. Grynkiewicz, G., Poenie, M., and Tsien, R. Y. (1985) A new generation of Ca^{2+} indicators with greatly improved fluorescence properties, *J. Biol. Chem. 260*, 3440−3450.
31. Spector, D. L., Fu, X. D., and Maniatis, T. (1991) Associations between distinct pre-messenger-RNA splicing components and the cell-nucleus, *EMBO J. 10*, 3467−3481.
32. Yoo, S. H., So, S. H., Kweon, H. S., Lee, J. S., Kang, M. K., and Jeon, C. J. (2000) Coupling of the Inositol 1,4,5-Trisphosphate Receptor and Chromogranins A and B in Secretory Granules, *J. Biol. Chem. 275*, 12553−12559.
33. Huh, Y. H., and Yoo, S. H. (2003) Presence of the inositol 1,4,5-trisphosphate receptor isoforms in the nucleoplasm, *FEBS Lett. 555*, 411−418.
34. Yoo, S. H., and Lewis, M. S. (1996) Effects of pH and Ca^{2+} on Hetetro-Dimer and Hetero-Tetramer Formation by Chromogranin A and Chromogranin B, *J. Biol. Chem. 271*, 17041−17046.
35. Choe, C. U., Harrison, K. D., Grant, W., and Ehrlich, B. E. (2004) Functional coupling of chromogranin with the inositol 1,4,5-trisphosphate receptor shapes calcium signaling, *J. Biol. Chem. 279*, 35551−35556.
36. Pimplikar, S. W., and Huttner, W. B. (1992) Chromogranin B (secretogranin I), a secretory protein of the regulated pathway, is also present in a tightly membrane-associated form in PC12 cells, *J. Biol. Chem. 267*, 4110−4118.
37. Rosa, P., Hille, A., Lee, R. W. H., Zanini, A., de Camilli, P., and Huttner, W. B. (1985) Secretogranins I and II: Two tyrosine-sulfated secretory proteins common to a variety of cells secreting peptides by the regulated pathway, *J. Cell Biol. 101*, 1999−2011.
38. Beuret, N., Stettler, H., Renold, A., Rutishauser, J., and Spiess, M. (2004) Expression of regulated secretory proteins is sufficient to generate granule-like structures in constitutively secreting cells, *J. Biol. Chem. 279*, 20242−20249.

BI048070W